Time Allocation Committee for
MPG time at the ESO 2.2m-telescope
c/o MPI für Astronomie
Königstuhl 17
D-69117 Heidelberg / Germany

Application No.	
Observing period	October 2020
Received	

APPLICATION FOR OBSERVING TIME

from [X] MPIA [ ] MPG institute [ ] other

1. Telescope: 2.2-m [X]

2.1 Applicant

Annika **Oetjens**	Max-Planck-Institute for Astronomy
Name	Institute
Koenigstuhl 17	69117 Heidelberg
street	ZIP code - city
	oetjens@mpia-hd.mpg.de
ESO User Portal username	e-mail

2.2 Collaborators

M.Bergemann, L.Carone, C.Hansen	Max-Planck-Institute for Astronomy
name(s)	institute(s)
R.Holcomb, A.Serenelli	University of California, ICE, CSIC, IEEC
name(s)	institute(s)

2.3 Observers

Annika Oetjens	Camilla Juul Hansen
name	name

By specifying the names under item 2.3 it is obligatory to also send out these observers to La Silla, if required. Correspondence on the rating of this application will be sent to the applicant (P.I.) as quoted under 2.1 above.

3. Observing programme: Category: [E]

Title : **How often does a planet spin-up its host star?**

Abstract : Recent studies highlight peculiar rotation velocities of old main-sequence stars, casting doubt on the universality of the canonical gyrochronology relation that ties the age of a star to its spin. We request FEROS spectra of 100 Galactic stars. With precise measurements of their rotation periods based on the TESS light-curves and accurate metallicities determined from the FEROS data, we can test the scenario of planet engulfment as the cause of abnormal stellar rotation velocities. The results of this study will shed new light on the frequency and chemical properties of stars that have experienced planet engulfment or are in a stable synchronized state with their planets.

4. Instrument: [ ] WFI [X] FEROS [ ] GROND

5. Brightness range of objects to be observed: from V=8.5 to V=11

6. Number of hours:

applied for			already awarded	still needed
28			none	none
no restriction	grey	dark		

7. Optimum date range for the observations: .... 1.10.2020 – 15.12.2020
Usable range in local sideral time LST: .... h – h

Astrophysical context

The age of a star is one of the most difficult astrophysical properties to derive from first principles. Asteroseismology is a powerful method, but it is currently limited to small spatial volumes in the Galaxy. An alternative is the famous gyrochronology relationship, which relates the rate of decay of stellar spin to age as $t^{-1/2}$ ([1]). However, recent studies suggest that the ages derived using these two methods show significant, of over 20%, discrepancies, even for some of the best-studied main-sequence stars [2]. The stars rotate too fast, compared to their age expectations based on asteroseismology. This implies that the canonical picture, in which the rotation period of a main-sequence star is solely controlled by the loss of angular momentum by magnetized stellar winds ([3], [4], [5]) misses some critical physics.

This paradox could be solved by considering the interaction between a star and its companion (a planet or a brown dwarf). Recent models that combine stellar structure with tidal migration and magnetic braking suggest that, as a consequence of angular momentum exchange, the stellar spin may change dramatically ([6], [7], [8]). A main-sequence star may spin up from a few kms^{-1} up to 40 kms^{-1} due to planet engulfment. The key observable prediction of our [7] model is that the frequency of stars experiencing this scenario increases with decreasing metallicity of a system.

Here we are requesting FEROS spectra for 100 rapidly-rotating main-sequence stars, which are likely metal-poor and old. These data will allow us to determine accurate chemical composition of these stars for the first time. In this way, we will test the main observable signature of our scenario, shedding new light on the frequency and chemical properties of stars that have experienced planet engulfment or are in a stable synchronized state with their planets.

Immediate aim

Our detailed dynamical model suggests that a fraction of metal-poor stars should show unexpectedly large, over ~ 5 kms^{-1}, rotation velocities, and that the rotation rates will show a systematic dependence on the mass and metallicity of a star (the relation is quantified in our recent study [7]).

We will test this prediction by quantifying the observed frequency and statistics of rapidly-rotating stars against their mass and metallicity. The FEROS spectra will give us a unique opportunity to do this now, as precision measurements of photometric rotation periods have just become available from the TESS (Transiting Exoplanet Survey Satellite) mission, whereas the data from the Gaia space mission allow to constrain the masses of our stars. Our model predictions in the parameter space of observables (mass, metallicity of stars) can be directly tested against the data obtained in this proposal.

Previous work

We have developed robust numerical techniques to analyse stellar spectra and determine accurate stellar parameters and metallicites with Non-LTE spectroscopic models (e.g. [9], [10]). The code to determine masses and ages of stars by means of isochrone fitting in the Bayesian framework was presented in [13]. The model describing the dynamical interaction of the star and its companion and the influence on the physical structure of a star was developed and discussed in detail in our earlier studies [6, 11, 7].

Target Selection

Stellar rotation periods were calculated from 2-minute cadence TESS light curves using a procedure similar to that outlined in [12]. In this method, rotation periods are identified by the locations of repeated peaks in the auto-correlation function of the light curve. This allowed us to identify and select bright $V_{\mathrm{mag}} < 12$ stars that are fast rotators ($P < 5$ days) and are expected to be metal-poor based on the preliminary (approximate) estimates of their metal content ([M/H]). When the latter estimates were not available, we preferentially selected bluer stars with a high B-V index.

Layout of observations

We need a representative sample of main-sequence stars broadly distributed in metallicity. Thus, we target 100 stars with $\mathrm{T}_{\mathrm{eff}} \sim 6000\,\mathrm{K}$ and log(g)> 4. We select bright southern stars (8 <V<$\sim$ 10.5). Those with with preliminary [M/H] are our high priority candidates, while stars with missing [M/H], but blue B-V colours, have been assigned medium priority. We require a high signal-to-noise in order to derive accurate metallicities and abundances of α-elements, so that the masses of our stars could be constrained as well. The targets are best observable between October and mid-December.

Strategic importance for MPIA

The project ideally meshes the research objectives in the PSF, GC, and APEX departments. We will provide accurate chemical composition of rapidly-rotating metal-poor stars, in order to test the existence of a peculiar population of stars, which may have experienced planet engulfment. The analysis will complement the efforts at MPIA to understand the chemistry of planet hosts (e.g., L. Kreidberg) and the dynamical interaction between proto-planetary discs, planets, and their host stars (e.g., B. Bitsch, L. Carone, M. Flock, T. Henning), as well as the chemical composition of stars and stellar populations in the Milky Way galaxy (e.g., M. Bergemann, N. Neumayer, H.-W.Rix). We are planning to present our results in a scientific article lead by the student Annika Oetjens.

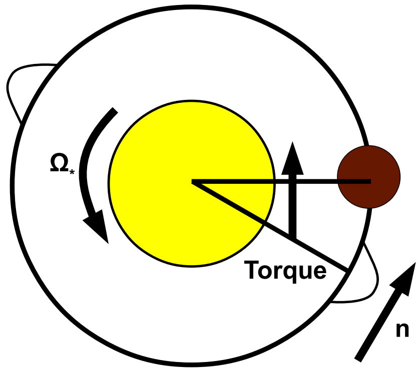

Figure 1: Angular momentum transfer during planetary engulfment due to tidal friction for a close-in heavy companion.

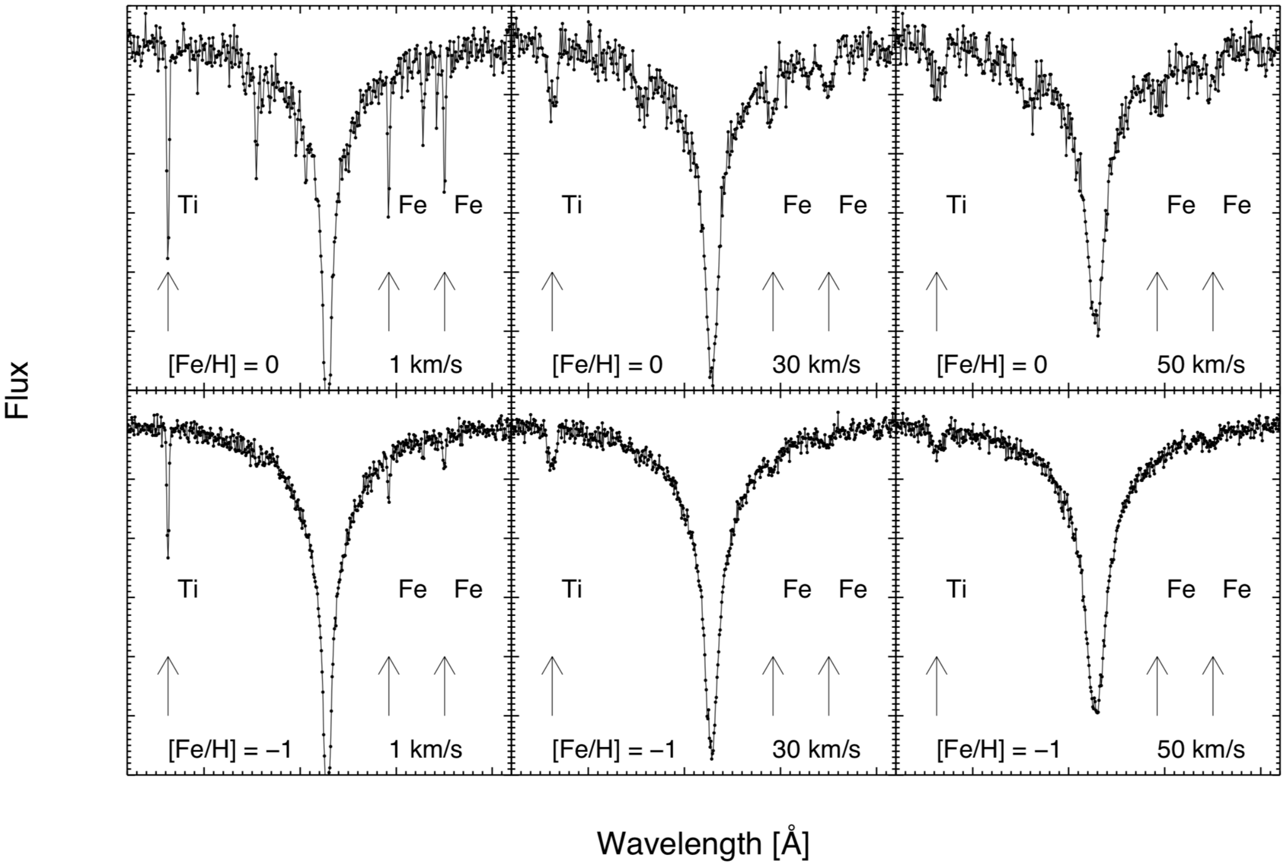

Figure 2: Simulations of stellar spectra for Sun-like model atmospheres with metallicity [Fe/H] = 0 (top panel) and −1 (bottom panel). The synthetic spectra are convolved with the rotation velocity of 1 $\mathrm{kms^{-1}}$ (left), 30 $\mathrm{kms^{-1}}$ (middle), and 50 $\mathrm{kms^{-1}}$ (right).

9. Objects to be observed

(Objects to be observed with high priority should be marked in last column)

Designation	α (2000)	δ (2000)	magnitude in spectral range to be observed	priority
139197342	$23^{h}\,2^{m}\,9.^{s}6730$	$-44^\circ\,16'\,45.3589''$	9.40000	high
142082604	$6^{h}\,33^{m}\,37.^{s}8520$	$-72^\circ\,16'\,35.0592''$	10.3390	high
143104637	$5^{h}\,57^{m}\,28.^{s}0573$	$-35^\circ\,0'\,9.80530''$	9.65100	high
144046583	$22^{h}\,27^{m}\,19.^{s}1464$	$-50^\circ\,4'\,20.0739''$	9.24800	high
144069454	$22^{h}\,31^{m}\,49.^{s}2384$	$-49^\circ\,10'\,31.0410''$	9.43900	high
150188659	$6^{h}\,14^{m}\,50.^{s}9998$	$-60^\circ\,48'\,54.8602''$	10.3180	high
161170644	$22^{h}\,38^{m}\,3.^{s}8104$	$-48^\circ\,45'\,33.5632''$	9.60000	high
177252917	$6^{h}\,46^{m}\,58.^{s}3777$	$-72^\circ\,12'\,35.8319''$	10.2360	high
206560410	$22^{h}\,15^{m}\,13.^{s}6642$	$-22^\circ\,50'\,30.5649''$	9.50700	high
279475335	$7^{h}\,0^{m}\,30.^{s}3755$	$-59^\circ\,11'\,4.10980''$	10.9620	high
300161962	$7^{h}\,16^{m}\,26.^{s}2307$	$-69^\circ\,2'\,57.8687''$	10.4210	high
31377175	$5^{h}\,33^{m}\,44.^{s}9176$	$-26^\circ\,7'\,19.9612''$	10.1490	high
314829171	$3^{h}\,31^{m}\,26.^{s}1955$	$-74^\circ\,19'\,28.2861''$	9.49300	high
370009865	$3^{h}\,7^{m}\,44.^{s}0994$	$-69^\circ\,53'\,29.7382''$	9.55300	high
38516117	$4^{h}\,10^{m}\,34.^{s}9548$	$-64^\circ\,47'\,50.7001''$	9.85400	high
38964363	$0^{h}\,44^{m}\,12.^{s}5842$	$-68^\circ\,43'\,48.2043''$	9.23300	high
7445518	$5^{h}\,26^{m}\,30.^{s}0770$	$-42^\circ\,5'\,37.6099''$	10.1230	high
77725497	$5^{h}\,9^{m}\,5.^{s}0935$	$-35^\circ\,9'\,55.4865''$	10.0310	high
169380520	$5^{h}\,6^{m}\,27.^{s}6972$	$-15^\circ\,49'\,30.3598''$	9.11900	medium
56181180	$4^{h}\,44^{m}\,38.^{s}5922$	$-7^\circ\,24'\,37.9444''$	9.42300	medium
286132427	$9^{h}\,46^{m}\,54.^{s}0003$	$-4^\circ\,17'\,53.1239''$	8.69000	medium
166874846	$3^{h}\,58^{m}\,39.^{s}2642$	$-31^\circ\,35'\,42.3615''$	9.43800	medium
152370762	$4^{h}\,21^{m}\,10.^{s}3199$	$-24^\circ\,32'\,21.1194''$	9.43300	medium
112931015	$7^{h}\,31^{m}\,30.^{s}2407$	$-34^\circ\,43'\,14.8746''$	9.08000	medium
167344043	$6^{h}\,34^{m}\,41.^{s}0390$	$-69^\circ\,53'\,6.36475''$	9.16800	medium
176317461	$4^{h}\,46^{m}\,44.^{s}5674$	$-5^\circ\,3'\,27.2159''$	9.50900	medium
13955147	$5^{h}\,0^{m}\,51.^{s}8641$	$-41^\circ\,1'\,6.60461''$	9.52000	medium
92845906	$5^{h}\,30^{m}\,19.^{s}0802$	$-19^\circ\,16'\,31.7976''$	9.53900	medium
24347173	$5^{h}\,16^{m}\,42.^{s}5763$	$-8^\circ\,42'\,14.9030''$	9.56100	medium
167486555	$4^{h}\,48^{m}\,27.^{s}6466$	$-10^\circ\,52'\,16.6791''$	9.42400	medium
393267642	$5^{h}\,47^{m}\,9.^{s}26285$	$-43^\circ\,7'\,14.8801''$	9.40000	medium
423830910	$4^{h}\,46^{m}\,7.^{s}96921$	$-27^\circ\,23'\,42.0016''$	9.59000	medium
425162657	$3^{h}\,55^{m}\,20.^{s}3998$	$-1^\circ\,43'\,45.1199''$	9.04200	medium
9266806	$4^{h}\,11^{m}\,11.^{s}0638$	$-3^\circ\,22'\,20.1003''$	9.47400	medium
248447740	$5^{h}\,11^{m}\,9.^{s}67163$	$-4^\circ\,10'\,54.4075''$	9.24400	medium
1529712	$5^{h}\,3^{m}\,33.^{s}8643$	$-33^\circ\,49'\,20.6369''$	9.52000	medium
442868242	$5^{h}\,19^{m}\,24.^{s}1680$	$-17^\circ\,44'\,53.1610''$	9.34900	medium
178938417	$4^{h}\,33^{m}\,6.^{s}24069$	$-24^\circ\,0'\,47.8798''$	9.05700	medium
409973553	$9^{h}\,41^{m}\,34.^{s}5591$	$-17^\circ\,53'\,11.3979''$	8.91800	medium
168753192	$4^{h}\,11^{m}\,52.^{s}2488$	$-30^\circ\,19'\,47.2787''$	9.21400	medium
401154449	$9^{h}\,0^{m}\,37.^{s}1990$	$-48^\circ\,59'\,28.3182''$	9.32000	medium
189013298	$5^{h}\,16^{m}\,14.^{s}2573$	$-15^\circ\,20'\,22.2015''$	9.24700	medium
60660469	$9^{h}\,13^{m}\,2.^{s}39822$	$-7^\circ\,33'\,17.8207''$	8.84000	medium
139827347	$4^{h}\,33^{m}\,17.^{s}3522$	$-20^\circ\,53'\,38.0397''$	9.55800	medium
281598849	$0^{h}\,36^{m}\,27.^{s}6720$	$-58^\circ\,12'\,33.1265''$	8.39000	medium
List truncated				

10. `Justification of the amount of observing time requested:`

Our targets are fairly bright, but owing to their somewhat fast rotation a signal-to-noise (S/N) of 100 is needed to detect and accurately measure the metallicity ([Fe/H]). We therefore need a high-resolution spectrograph, to resolve the lines and avoid blended features. With a lot of Fe lines located throughout the spectrum, we set the S/N at 5000Å so that we can also derive accurate stellar parameters from the spectra. This guarantees that we can derive stellar parameters and metallities to an accuracy of ± 0.1 dex. As the targets are mainly dwarfs/ main sequence stars with an average temperature of 6000 K, we use the FEROS ETC v. 106.1 to estimate the needed exposure times. As the targets are bright, we can observe at a seeing of 1.3 arcsec, airmass of ~ 1.5 and fairly bright moon conditions (we used FLI=0.7). We select a 1x1 binning and fast readout. This leads to the following exposure times at 5000Å (not including overhead):

Vmag=8.5 $\rightarrow$ 200s, Vmag=9.5 $\rightarrow$ 500s, Vmag=10.5 $\rightarrow$ 900s

Our sample with well-constrained stellar parameters (18 stars) therefore needs 12000s on target and another 8640s overhead (assuming 8min per target). The sample without known [Fe/H] but blue colours and similar temperatures (82 stars) are centered on Vmag=8.5-9.5 and on average need 500s per target and results in 41000s plus 39360s overhead. We need a statistically significant sample in order to observationally probe the relation between rotation and engulfment, and hence we request a total of **28h**.

11. `Constraints for scheduling observations for this application:`

12. `Observational experience of observer(s) named under 2.3:`
    `(at least one observer must have sufficient experience)`

Mar 2020 – UVES/VLT ESO, Chile: Co-I (2n - visitor mode)
Apr 2013 – HDS/Subaru, Mauna Kea, Hawaii, US: Co-I (1n $\sim$10h - visitor mode)
Aug 2010 – X-Shooter/VLT ESO, Chile: Co-I (1.5n $\sim$15h - visitor mode)
Jul 2006 – AURELIE/OHP, Observatoire de Haute Provence, France: Co-I (5n - visitor mode)
2004 – Brorfelde Schmidt telescope, Brorfelde Observatory, Denmark: Co-I (1n - visitor mode)
2008 – 2020: High-resolution spectroscopy, world wide including PEPSI and FEROS: PI or Co-I - $> 200h$ service mode

13. `Observing runs at the ESO 2.2m-telscope (preferably during the last 3 years)`
    `and publications resulting from these`

Telescope	instrument	date	hours	success rate	publications

14. References for items 8 and 13:

[1] Skumanich, A. 1972, ApJ, 171, 565

[2] Sahlholdt, C. L., Feltzing, S., Lindegren, L., Church, R. P. 2019, MNRAS, 482, 895

[3] Bouvier, J., Forestini, M., & Allain, S. 1997, A&A, 326, 1023

[4] Barnes, S. A. 2003, ApJ, 586, 464

[5] Angus, R., Morton, T. D., Foreman-Mackey, D., et al. 2019, AJ, 158, 173

[6] Carone, L. & Pätzold, M. 2007, Planet. Space Sci., 55, 643

[7] Oetjens et al. subm.

[8] Bolmont, E., Gallet, F., Mathis, S., et al. 2017, A&A, 604, A113

[9] Bergemann, M., Lind, K., Collet, R., et al. 2012, MNRAS, 427, 27

[10] Bergemann, M., Collet, R., Amarsi, A. M., et al. 2017, ApJ, 847, 15

[11] Carone, L. 2012, PhD thesis, Universität Köln, https://kups.ub.uni-koeln.de/4757/

[12] Saylor D. A., Lépine S., Crossfield I. and Petigura E. 2018, AJ, 155, 23

[13] Serenelli, A. M., Bergemann, M., Ruchti, G., Casagrande, L. 2013, MNRAS,429, 3645

[14] Nielsen, M. B., Schunker, H., Gizon, L., Ball, W. H. 2015, A&A, 582, A10

Tolerance limits for planned observations:

maximum seeing: 1.3″	**minimum transparency:** %	**maximum airmass:** 1.5
photometric conditions: no	**moon: max. phase / ∠ :** 0.7/30°	**min. / max. lag:** / nights